

Radiation from Cerenkov Wakes in a Magnetized Plasma

J. Yoshii, C. H. Lai, and T. Katsouleas

University of Southern California, Department of Electrical Engineering, Electrophysics, Los Angeles, California 90089-0484

C. Joshi and W. B. Mori

University of California, Los Angeles, Department of Electrical Engineering, Los Angeles, California 90024

(Received 26 February 1997)

The Cerenkov wake excited by a particle beam or a short laser pulse in a perpendicularly magnetized plasma is analyzed. The wake couples to electromagnetic radiation of approximate frequency ω_p at the plasma/vacuum boundary. The radiation amplitude is ω_c/ω_p times the amplitude of the wake excited in the plasma (for a sharp boundary). Particle-in-cell simulations verify the scaling laws. Since plasma wakes as high as a few GeV/m are produced in current experiments, the potential for a high-power (i.e., GW) coherent microwave to THz radiation source exists. [S0031-9007(97)04526-2]

PACS numbers: 52.40.Mj, 41.60.Bq, 52.40.Nk, 52.75.Va

Recently there have been a number of experiments on the use of intense pulses of electron or laser beams to excite large-amplitude (up to 100 GeV/m) plasma wakes [1–5]. These wakes can be used to accelerate particles at ultrahigh rates or to generate THz radiation [6]. In this Letter, we consider the use of a dc magnetic field to couple the electrostatic wakes to electromagnetic radiation that can propagate out of plasma. This radiation may be valuable as a diagnostic for the plasma accelerator experiments or as a source of high-power tunable coherent radiation in the submillimeter wave range.

It is well known that an electrostatic plasma oscillation near the plasma frequency ω_p can radiate an electromagnetic wave at the same frequency by inverse mode conversion [7]. As this radiation is near cutoff, it is strongly absorbed by the plasma unless the plasma itself is on the order of a skin depth (c/ω_p) wide. In this case the plasma wave acts as a dipole antenna, oscillating in the direction of k of the wave, and the electromagnetic (EM) radiation escapes the plasma in a plane primarily perpendicular to this direction.

We consider instead the radiation produced by a plasma wake in a perpendicular dc magnetic field. As in the unmagnetized case, the radiation is near the plasma frequency and, thus, is tunable by varying the plasma density. However, the addition of an applied magnetic field significantly alters the scenario. First, unlike the unmagnetized wake which is electrostatic [8], the magnetized wake field has both electromagnetic ($\mathbf{k} \times \mathbf{E} \neq 0$) and electrostatic ($\mathbf{k} \cdot \mathbf{E} \neq 0$) components. Second, unlike the cold unmagnetized plasma wake, the magnetized wake has a nonzero group velocity. This enables the wake to propagate through the body of the plasma to the edge and to couple radiation into the vacuum. Thus, much larger output power is obtainable since wake energy from a larger volume can be coupled to radiation outside the plasma. Third, the radiation is primarily in a small solid angle in the forward direction rather than radially directed in 2π . In this Letter, wakes excited by either short pulse laser or

particle beams are considered and modeled with particle-in-cell (PIC) simulations. For wake field drivers currently in use for plasma accelerator applications, the results suggest that application of an appropriate magnetic field could result in production of GHz to THz radiation at power approaching GW levels.

The geometry of the radiation scheme considered here is shown in Fig. 1. A short pulse (or train of pulses) of particle or laser beam propagates at nearly the speed of light in the $+x$ direction. A dc magnetic field exists in the $+z$ direction; for simplicity we take this to be uniform in space and constant in time.

To understand the expected radiation, consider the diagrams in Fig. 2 illustrating the Cerenkov angle and the infinite cold magnetized plasma dispersion relation. As is well known [9], Cerenkov resonance occurs at the angle $V_b \cos \theta = \omega/k$ as shown in Fig. 2(a). Here, V_b is the velocity of the disturbance that creates the wake in the medium (equal to the beam velocity for a particle beam or to the group velocity for a laser pulse). The intersection of this condition and the plasma dispersion curves shows the radiation that can be effectively excited at any given angle. This is shown, for $\theta = 0$ and $\theta > 0$, in Fig. 2(b) for $V_b \approx c$. At $\theta = 0$, the straight line intersects the lower branch of the extraordinary (XO) mode [10] at $\omega \approx \omega_p$. At this point the group velocity $V_g = d\omega/dk = (\omega_c^2/\omega_h^2)c$, where $\omega_c = eB_0/m_e c$ is the electron frequency and $\omega_h = (\omega_p^2 + \omega_c^2)^{1/2}$ is the hybrid

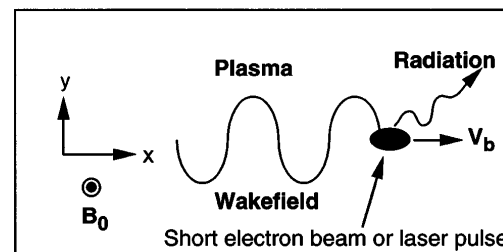


FIG. 1. Geometry for Cerenkov radiation generation.

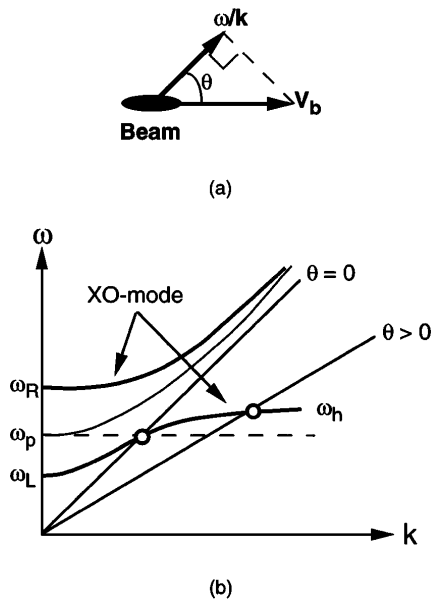


FIG. 2. Cerenkov wakes are produced at the intersection of (a) the Cerenkov condition ($V_b \cos \theta = \omega/k$) and (b) the plasma dispersion curves, where $\omega_R = [\omega_c + (\omega_c^2 + 4\omega_p^2)^{1/2}]/2$ and $\omega_L = [-\omega_c + (\omega_c^2 + 4\omega_p^2)^{1/2}]/2$.

frequency. The dispersion tensor [11] ϵ dotted with \mathbf{E} gives the ratio $|E_y/E_x| = \omega_c/\omega_p$ at $\omega = \omega_p$. Note that for $\omega_c = 0$, $E_y = 0$ (for infinitely wide plane waves) and the wake consists of purely electrostatic plasma oscillations at ω_p . Since $V_g = 0$ for a cold unmagnetized plasma, the drive pulse leaves behind its path a wake of parallel wave fronts ($\vec{k} = k\hat{x}$) that do not spread. In a magnetized plasma, the wake fronts on the x axis are similar. However, as seen from the $\theta > 0$ line in Fig. 2(b), there is a nonzero group velocity at other angles θ enabling the wake to spread transversely. The group velocity and wavelength ($2\pi/k$) are largest on axis ($\theta = 0$) and approach zero at $\theta = 90^\circ$. Thus, most of the wake energy travels forward.

To determine the power transmitted through the plasma/vacuum boundary, we have solved the boundary value problem at the interface. First, for a sharp boundary, by a straightforward application of the continuity of the tangential components of \mathbf{E} and \mathbf{B} to a system of plane incident, reflected and transmitted waves, we find that the transmitted wave has a transmission coefficient of one. That is, the transmitted wave has a transverse field (E_y) equal to the electromagnetic (E_y) component of the wake in the plasma. Moreover, the reflection coefficient is zero, and all of the wake energy is ultimately transmitted. This rather counter-intuitive result is more understandable when one considers that $\omega/k = c$ for the plasma wake as well as for the radiation in vacuum, so there is not a discontinuity of the refractive index (ck/ω) for this special case of frequency and wave number.

For continuous boundary cases, the Cerenkov wake will tunnel through an evanescent layer between the

upper and lower branch of the XO mode [10] as it propagates into the vacuum. The attenuation of the Cerenkov wake in the evanescent layer can be estimated as follows. For simplicity we assume a linear plasma density ramp of length L . Thus, we can write $\omega_p(x)^2 = \omega_{p0}^2(L-x)/L$. We note that the wake encounters the evanescent layer when $\omega_h(x) < \omega_{p0} < \omega_R(x)$, where $\omega_h(x) = [\omega_p(x)^2 + \omega_c^2]^{1/2}$ and $\omega_R(x) = \{\omega_c + [\omega_c^2 + 4\omega_p(x)^2]^{1/2}\}/2$. The total decay of the electric field can be calculated by integrating the imaginary k_i over the layer: $\Gamma = e^{-\int k_i dx}$, where k_i is obtained from the dispersion relation of the XO mode [10]. The result for a linear density ramp is $\Gamma = e^{\alpha L \omega_{p0}/c}$, where α is given by

$$\alpha = -\left(\frac{1}{\omega_p^3}\right) \int_{\omega_c^2 - \omega_{p0}\omega_c}^0 \sqrt{\frac{(z - \omega_c^2 - \omega_{p0}\omega_c)(z - \omega_c^2 + \omega_{p0}\omega_c)}{z}} dz. \quad (1)$$

α is plotted as a function of ω_c/ω_p in Fig. 3. This shows that the attenuation is greatest for $\omega_c/\omega_p \approx 0.65$. We comment that the evanescent layer can be reduced or even eliminated by suitable tailoring of the magnetic field in the ramped region. This will be the subject of future work.

With the transmission coefficient and the decay factor known, approximate scaling laws for the power radiated can be obtained from well known wake field theory results [12]. The average power density radiated in vacuum is simply

$$p = \frac{cE_y^2}{8\pi} \approx (\Gamma)^2 \left(\frac{\omega_c}{\omega_p}\right)^2 \frac{cE_x^2}{8\pi}. \quad (2)$$

The longitudinal wake field E_x can be estimated from 1D unmagnetized plasma theory [13]. For a short driving electron beam of density n_b and length $\pi c/\omega_p$, the amplitude of E_x is given by

$$E_x = (mc\omega_p/e)(n_b/n_0). \quad (3)$$

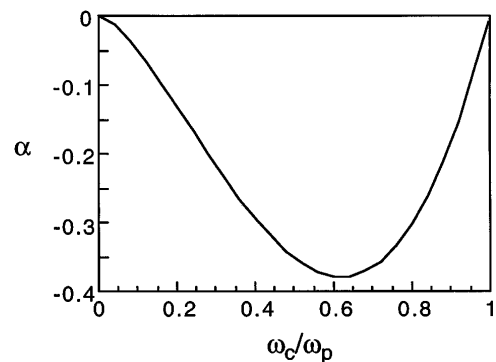


FIG. 3. Damping coefficient vs ω_c/ω_p from Eq. (1).

For a short laser pulse of normalized amplitude $V_{\text{osc}}/c = eE_0/m\omega_0c$ and pulse length $\pi c/\omega_p$, it is

$$E_x = (mc\omega_p/e) \frac{1}{2} \left(\frac{V_{\text{osc}}}{c} \right)^2. \quad (4)$$

For a train of pulses [14] or beating lasers, the amplitude may be found by integrating Eq. (4) up to a saturation value determined by relativistic detuning [15], modulational instabilities [16], or wave breaking [17].

The qualitative and quantitative features just described are next tested with fully self-consistent, relativistic 1D PIC simulations. The code used is WAVE. The wake fields excited in a 1D simulation are shown in Fig. 4. In this case, the driving beam was a short electron beam of peak density $n_b = 0.1n_0$ and full width at half maximum (FWHM) of $0.2c/\omega_p$ moving in the $+x$ direction with Lorentz factor $\gamma = 10^5$. In each case of Fig. 4, a plasma/vacuum boundary is centered at $x = 30c/\omega_p$. In case (a) there is an abrupt boundary; while in (b) and (c), the density ramps down linearly from $n = n_0$ to zero over $10c/\omega_p$ and $20c/\omega_p$, respectively. At the time of Fig. 4, the beam has already exited the right hand boundary of the simulation. A constant magnetic field with strength corresponding to $\omega_c/\omega_p = 0.1$ is in the $+z$ direction. The longitudinal wakes E_x are shown for each case on the left side of Fig. 4 and the transverse components E_y are shown on the right. We comment that E_x is nearly identical to the E_x observed in the unmagnetized simulations. Without the magnetic field, $E_y = 0$ in 1D. With the magnetic field, the amplitude of E_y in the plasma is approximately ω_c/ω_p times E_x as expected from the dispersion relation. The electrostatic wave component E_x vanishes as expected in the vacuum region and develops a short wavelength structure in the ramped region. This short wavelength structure is

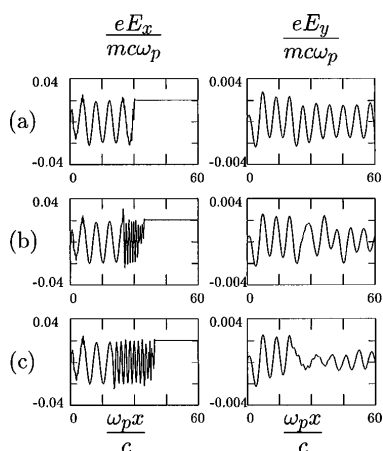


FIG. 4. 1D PIC simulations of Cerenkov wake fields. The longitudinal (transverse) electric field component is shown on the left (right). In case (a), a sharp plasma/vacuum boundary is at $x = 30c/\omega_p$; in case (b), the plasma density ramps linearly to zero from $x = (25-35)c/\omega_p$; in case (c), the ramp is from $(20-40)c/\omega_p$.

simply the result of the local plasma electrons oscillating with the local plasma frequency in each region. These oscillations become out of phase causing the phase variation seen in the ramped region. Over time the wavelengths become shorter and shorter (not shown) and ultimately Landau damp as their phase velocities decrease toward the plasma's thermal velocity. The behavior of the electromagnetic component is quite different. We have observed in simulations that an electromagnetic wave propagates in the vacuum region with an amplitude roughly equal to that of the E_y component in the plasma in the case of a sharp boundary [see Fig. 4(a)]. For the continuous boundary cases [Figs. 4(b) and 4(c)], we observe that the transmitted radiation through the plasma/vacuum boundary is smaller than in the sharp boundary case as expected from Eq. (1). For case 4(b), E_{trans}/E_y is 0.6, while for case 4(c), it is 0.4; Eq. (1) predicts $E_{\text{trans}}/E_y = 0.6$ and 0.37, respectively.

The simulation snapshots in Fig. 4 are at $t = 100\omega_p^{-1}$. We have observed that even though only a few (N) wake cycles are excited in the simulation box, the electromagnetic radiation is generated for a much longer time. This is due to the lower group velocity of the wake, which causes it to be left behind the driver, "ringing" for a time given by $N \times 2\pi c/\omega_p V_g$ or a plasma oscillation damping time, whichever is smaller. Substituting for V_g and assuming weak damping, we can obtain the duration of the radiation $\tau \approx 2\pi N \omega_h^2/\omega_p \omega_c^2 \approx L_p \omega_h^2/c \omega_c^2$, where L_p is the length of the plasma. It is interesting to note that only a small fraction (ω_c^2/ω_p^2) of the wake field energy is associated with the electromagnetic component (for small ω_c/ω_p); most of it is in the longitudinal plasma motion (field and kinetic energy). The wake energy as a whole conserves power flux at the boundary, as it can be easily verified that $v_g[(E_x^2 + E_y^2 + B_z^2)/16\pi + 1/2n_0m(\bar{v}_x^2 + \bar{v}_y^2)]$ in the plasma is equal to $c(E_y^2/8\pi)$ in vacuum.

We have also used the PIC simulations to verify the scaling law [Eq. (2)] over a range of ω_c/ω_p from zero to about 0.8 for the sharp boundary cases. Figure 5 shows the amplitude of E_y normalized to E_{x0} (the unmagnetized longitudinal wake amplitude) in plasma vs ω_c/ω_p . It is interesting that at large ω_c/ω_p the wakes look very different from those in Fig. 4. Because of the larger group velocity at high ω_c/ω_p , the wake tends to follow the driver rather than being left behind. As ω_c/ω_p gets larger, the wake becomes more and more like the bow shock wake around a bullet in air.

Up to now, we have considered only one-dimensional effects, which we expect to be valid for driving beams that are wide compared to a plasma wavelength ($2\pi c/\omega_p$) [18]. Indeed, in 2D PIC simulations that we have performed of wakes a couple of wavelengths wide, the radiation amplitude is almost identical to that in the 1D runs. However, several new effects occur for beams of modest width. First, the wake has both longitudinal and transverse electrostatic components; these are known in plasma

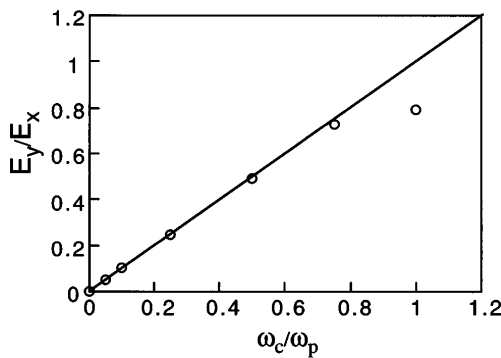


FIG. 5. Transverse electric field in plasma as a function of ω_c/ω_p normalized to longitudinal electric field in unmagnetized plasma in 1D plasma simulations. Straight line is from linear dispersion theory.

wake field accelerators as accelerating and focusing fields. E_y/E_x due to the B field scales as ω_c/ω_p , while E_y/E_x from electrostatic focusing scales as $1/k_p\sigma_r$, where σ_r is the width of the wake. Thus, we expect the transverse radiation field to dominate the transverse electrostatic contribution in the plasma when $k_p\sigma_r \gg \omega_p/\omega_c$. Second, the nonzero group velocity in the transverse direction causes some wake energy to propagate out sideways rather than forward. The wake energy propagates away from axis (x) asymmetrically since wakes with $k = k_y$ are perpendicular to B_0 , while wakes with the same value of k in the z direction are oblique to B_0 and therefore satisfy a modified dispersion relation. Third, if transverse plasma boundaries are nearby (within c/ω_p), the plasma wake radiates sideways from surface currents near the boundary [6].

To illustrate the scaling law [Eq. (2)], we take two examples from current plasma accelerator experiments. The first is a particle beam driven wake field experiment [19]. The driving beam consists of $N = 6 \times 10^9$ (1 nC) electrons in a $0.5\lambda_p$ long bunch with a radius of $300 \mu\text{m}$. For a plasma density $n_0 = 10^{14} \text{ cm}^{-3}$, $n_b/n_0 \approx 0.04$ and the expected wake amplitude is $E_x = 40 \text{ MV/m}$. For a dc magnetic field of 3.6 kG ($\omega_c/\omega_p = 0.1$), the scaling law Eq. (2) predicts an output power of 2 kW at frequency $\omega_p/2\pi = 100 \text{ GHz}$ for a sharp boundary. As a second example, consider the parameters of a recent beatwave accelerator experiment at UCLA [20]. A plasma of density $n_0 = 10^{16} \text{ cm}^{-3}$ was driven by two CO_2 laser lines ($\lambda = 10.6$ and $10.3 \mu\text{m}$) such that their beat frequency was resonant with ω_p . Based on Thompson scattering and other diagnostics, a plasma wake of amplitude $E_x \approx (0.3-0.5)mc\omega_p/e$ was excited over a 1 cm length. Equation (2) predicts that an imposed magnetic field of $B_0 = 180 \text{ kG}$ ($\omega_c/\omega_p = 0.5$) could cause the wake to radiate approximately 1 GW of power at a frequency of $\omega_p/2\pi \approx 1 \text{ THz}$ for a sharp boundary. A more modest magnetic field of only 6 kG appears to be sufficient to produce one MW power levels.

Further work is needed to obtain the angular and frequency distribution of the output power as well as its efficiency. Other geometries and magnetic field directions are also of interest. Further work may lead to a unique source of high-power coherent radiation.

This Letter was supported in part by U.S. DOE under Grant No. DE-FG03-92ER40745 and by AFOSR under Grant No. F49620-95-1-0248. Some of the authors have benefited from conversations with Garnick Hairapetian and Ronglin Liou.

- [1] Special Issue on Second Generation Plasma Accelerators, edited by T. Katsouleas and R. Bingham [IEEE Trans. Plasma Sci. **24**, No. 2 (1996)].
- [2] A. Modena *et al.*, Nature (London) **377**, 606 (1995); D. Umstadter *et al.*, Science **273**, 472 (1996).
- [3] F. Amiranoff *et al.*, in Ref. [1].
- [4] J.R. Marques *et al.*, Phys. Rev. Lett. **76**, 3566 (1996); K. Nakajima *et al.* (private communication); C. Seders *et al.*, Phys. Rev. Lett. **76**, 3570 (1996).
- [5] J. Rosenzweig *et al.*, Phys. Rev. Lett. **61**, 98 (1988).
- [6] H. Hamster *et al.*, Phys. Rev. Lett. **71**, 2725 (1993).
- [7] V.L. Ginzburg, *The Propagation of Electromagnetic Waves in Plasmas* (Pergamon Press, New York, 1970).
- [8] In linear theory the plasma wakes are electrostatic. Recently it was shown that these wakes contain second order electromagnetic terms by L. Gorbunov, P. Mora, and T. Antonsen, Phys. Rev. Lett. **76**, 2495 (1996).
- [9] Cerenkov radiation in magnetized plasmas has been studied, for example, in the case of runaway electrons in tokamak plasmas by I.H. Hutchinson *et al.*, Phys. Fluids **23**, 1698 (1980); Phys. Rev. Lett. **54**, 800 (1985); Phys. Fluids **26**, 310 (1983); Phys. Fluids **28**, 1090 (1985).
- [10] Francis F. Chen, *Introduction to Plasma Physics and Controlled Fusion, 1* (Plenum Press, New York, 1984), 2nd ed.
- [11] T.H. Stix, *Waves in Plasmas* (AIP Press, New York, 1992).
- [12] For a detailed review, see E. Esarey *et al.*, in Ref. [1], p. 252.
- [13] W.B. Mori, C. Joshi, and J.M. Dawson, IEEE Trans. Nucl. Sci. **30**, 3244 (1983).
- [14] D. Umstadter, E. Esarey, and J. Kim, Phys. Rev. Lett. **72**, 1224 (1994).
- [15] C.M. Tang, P. Sprangle, and R. Sudan, Appl. Phys. Lett. **45**, 375 (1985); M. Rosenbluth and C.S. Liu, Appl. Phys. Lett. **29**, 701 (1972).
- [16] F. Amiranoff *et al.*, Phys. Rev. Lett. **68**, 3710 (1992).
- [17] W.B. Mori and T. Katsouleas, Phys. Scr. **T30**, 127 (1990).
- [18] R. Keinigs and M.E. Jones, Phys. Fluids **30**, 252 (1987); P. Sprangle *et al.*, Appl. Phys. Lett. **53**, 2146 (1988); R. Fedele *et al.*, Phys. Rev. A **33**, 4412 (1986).
- [19] C. Joshi *et al.*, (private communication).
- [20] C.E. Clayton *et al.*, Phys. Rev. Lett. **70**, 37 (1993).